Environmental Science Processes & Impacts

ROYAL SOCIETY OF CHEMISTRY

PAPER

View Article Online
View Journal | View Issue



Cite this: *Environ. Sci.: Processes Impacts*, 2021, **23**, 1146

# Introducing a nested multimedia fate and transport model for organic contaminants (NEM)†

Knut Breivik, *[ab] Sabine Eckhardt,[a] Michael S. McLachlan [c] and Frank Wania [d]

Some organic contaminants, including the persistent organic pollutants (POPs), have achieved global distribution through long range atmospheric transport (LRAT). Regulatory efforts, monitoring programs and modelling studies address the LRAT of POPs on national, continental (*e.g.* Europe) and/or global scales. Whereas national and continental-scale models require estimates of the input of globally dispersed chemicals from outside of the model domain, existing global-scale models either have relatively coarse spatial resolution or are so computationally demanding that it limits their usefulness. Here we introduce the Nested Exposure Model (NEM), which is a multimedia fate and transport model that is global in scale yet can achieve high spatial resolution of a user-defined target region without huge computational demands. Evaluating NEM by comparing model predictions for PCB-153 in air with measurements at nine long-term monitoring sites of the European Monitoring and Evaluation Programme (EMEP) reveals that nested simulations at a resolution of 1° × 1° yield results within a factor of 1.5 of observations at sites in northern Europe. At this resolution, the model attributes more than 90% of the atmospheric burden within any of the grid cells containing an EMEP site to advective atmospheric transport from elsewhere. Deteriorating model performance with decreasing resolution (15° × 15°, 5° × 5° and 1° × 1°), manifested by overestimation of concentrations across most of northern Europe by more than a factor of 3, illustrates the effect of numerical diffusion. Finally, we apply the model to demonstrate how the choice of spatial resolution affect predictions of atmospheric deposition to the Baltic Sea. While we envisage that NEM may be used for a wide range of applications in the future, further evaluation will be required to delineate the boundaries of applicability towards chemicals with divergent fate properties as well as in environmental media other than air.

Received 20th February 2021
Accepted 29th June 2021

DOI: 10.1039/d1em00084e

rsc.li/espi



### Environmental significance

Within a regulatory context, the model-based assessment of the potential of organic chemical for long range atmospheric transport (LRAT) is often accomplished with extremely simple models lacking spatial resolution. The computational efficiency of the nested global modelling approach introduced here should enable future model applications of regulatory and scientific interest that previously were not possible with highly spatially resolved models. This includes (i) the performance of stochastic sensitivity and uncertainty analyses, (ii) the screening of large numbers of organic chemicals for LRAT, (iii) the modelling of complex contaminant mixtures comprised of numerous constituents with divergent LRAT potential, and (iv) model investigations requiring the simulation of large numbers of scenarios.

## Introduction

Persistent Organic Pollutants (POPs) have been banned and restricted globally because of possible harm to environment and human health.[1,2] The justification for their regulation on a global scale is their ability to undergo long-range environmental transport (LRT),[1,3,4] which has been established through numerous measurements at remote background sites[5,6] on national,[7–9] regional,[10,11] continental[12–15] and global scales.[16] Field measurements across geographical scales have been paralleled by regulatory efforts across national boundaries and jurisdictions. At the same time a wide variety of mathematical models has been developed to predict the environmental dispersal of POPs, because a comprehensive understanding of their long-range atmospheric transport (LRAT) and the consequences for sound control strategies cannot be achieved on the basis of measurements alone.

[a]*Norwegian Institute for Air Research, P.O. Box 100, NO-2027, Kjeller, Norway. E-mail: kbr@nilu.no; Tel: +47 63 89 80 00*

[b]*Department of Chemistry, University of Oslo, P.O. Box 1033, NO-0315, Oslo, Norway*

[c]*Department of Environmental Science, Stockholm University, SE-106 91, Stockholm, Sweden*

[d]*Department of Physical and Environmental Sciences, University of Toronto Scarborough, 1265 Military Trail, Toronto, Ontario, M1C 1A4, Canada*

† Electronic supplementary information (ESI) available: Table S1 and Fig. S1–S10. See DOI: 10.1039/d1em00084e

Because POPs reach remote areas mainly by LRAT, networks have been set up to measure their concentrations in air in support of national, regional and global policy objectives.[17] The most comprehensive network in Europe is the European Monitoring and Evaluation Programme (EMEP),[18] which collates POP measurements carried out by national laboratories as part of national programs. Similar arrangements apply to other regional long-term monitoring programs, such as the Arctic Monitoring and Assessment Programme (AMAP),[19] and the joint US-Canadian Great Lakes Integrated Atmospheric Deposition Network (IADN).[20] These programs have generated long-term time trends of POPs in the atmosphere based on data reaching back to the early 1990s. On a global scale, the Global Monitoring Plan (GMP) supports the implementation and effectiveness evaluation of the Stockholm Convention on POPs[1,21] by synthesizing data on ambient concentrations in air from national, regional and global air monitoring programs.[16,22]

Monitoring data do not only inform regulatory efforts but are also essential for model evaluations. In the context of LRAT, the utility of multimedia fate and transport models (MFTMs) targeting national scales[23,24] is limited. Continental-scale MFTMs such as Impact 2002 (ref. 25) or the Berkley-Trent models for North America[26,27] and Europe[28] suffer from difficulties in accurately defining the advective import of POPs from outside the model domain.[29] This is not an issue for global MFTMs which range from relatively simple evaluative models *e.g.*[30] to dynamic geo-referenced three-dimensional models.[31] Whereas MFTMs rely on simplified descriptions of environmental transport, such as meteorological conditions averaged over the time scale of a month, global high resolution transport models (HRTMs) account for the spatially and temporally highly dynamic nature of atmospheric mixing and removal processes. HRTMs are, for example, capable of realistically predicting the short-term variability in concentrations in air of remote regions,[32–34] such as the occurrence of LRAT episodes causing temporary concentration peaks.[35] At the same time, HRTMs tend to be computationally too demanding to simulate a wide range of POPs over the decadal time scales reflective of their environmental persistence.

Major challenges therefore still remain in terms of formulating models which have global coverage, high spatial resolution, and the capability of performing a large number of simulations (*e.g.* for multiple chemicals and scenarios or for sensitivity analyses). In other words, LRAT models which operate across scales to serve multiple needs are largely missing. We propose to address this need through a flexible, nested modelling approach which is (i) less computationally demanding, enabling numerous simulations at coarse resolution, (ii) able to individually target, yet also integrate regional, continental and global scales, (iii) offers higher spatial resolution of receptor regions of scientific and/or regulatory interest, and (iv) dynamic, allowing one to address the environmental response to changes in emissions.

The main objectives of this study are to (i) introduce a new Nested Exposure Model (NEM) for organic contaminants that is designed to meet those requirements, (ii) evaluate different geometries of the model by comparing predictions of variable resolution with each other and with measurements, (iii) apply the model to quantify the relative importance of local sources and advective atmospheric import from elsewhere to the concentrations observed in areas in which European background monitoring stations are located, and (iv) explore how the choice of spatial resolution affect predictions of atmospheric deposition to a specific receiving environment. PCB-153 is used as an example.

## Materials and methods

### Points of departure

NEM builds upon CoZMo-POP2 (ref. 36) and BETR-Global,[37] two existing dynamic MFTMs for predicting the long-term behavior of persistent semi-volatile organic contaminants in the physical environment. Whereas CoZMo-POP2 is not spatially resolved,[36] the resolution of the global-scale BETR-Global was originally 15° × 15° (lat/long),[31] but recently increased to 3.75°.[38] As all resolutions used here are identical in latitude and longitude we used $X°$ when referring to $X° \times X°$ in the remainder of the paper. NEM adopts major parts of the code from CoZMo-POP2 and supplements it with parts of the parameterization of BETR-Global.[38] An advantage of this approach is that these models have undergone extensive evaluations over the years lending credibility to the underlying process descriptions built into NEM. CoZMo-POP2 has been evaluated for PCBs[39] and short-chain chlorinated paraffins.[40] Similarly, BETR-Global has been previously evaluated and applied.[37,38] By relying on previously documented models and process descriptions, we can restrict the model documentation to those elements of NEM that are novel and make it different from CoZMo-POP2 and BETR-Global.

### Nesting

A key feature of NEM is the opportunity to operate the model across different spatial scales and resolutions to focus on a specific region of the globe. By nesting up to five different model domains with user-defined geometries and resolutions, NEM offers increasing resolution with increasing proximity to a given target region of interest. Through sequential calculations, model output obtained from simulating a larger domain with coarse resolution serves to define the boundary conditions for a smaller domain with finer resolution, nested within the larger domain. The nested domain needs to be fully incorporated within the larger domain and rely on boundary conditions derived from one preceding domain alone. This nested approach not only reduces computational demands by limiting simulations at the finest resolution to a user-defined region of interest, but it also allows for the assessment of the impact of spatial resolution on model predictions, all within a consistent modelling framework. The BETR-Global model relies on spatially variable environmental input data.[41] Most of these data sets have been replaced by new global databases as described and summarized below.

### Transport

Chemical transport between adjacent grid cells within NEM may occur by air, fresh water and seawater, and is defined on

the basis of data with a monthly temporal resolution and a 0.5° spatial resolution (Fig. S1†). NEM linearly interpolates monthly into daily values. Monthly means of fresh water discharge for the years 2000–2009 are taken from the global freshwater model WaterGAP 2.2c.[42] Freshwater flow from a grid cell may occur in eight directions (N, NE, E, SE, S, SW, W, NW) and vertically (inland sinks). Inland sinks are treated as an input of chemical to terrestrial surface media. Outflow cells for run-off into the sea are based on Döll *et al.*[43] Ocean circulation is based on the third version of the Simple Ocean Data Assimilation (SODA3) ocean reanalysis[44] for which the horizontal velocities in four directions (N, E, S, W) within the ocean mixing layer and the vertical velocity out of the mixing layer were retrieved (SODA 3.4.2, 30th May 2019). The parameterization of atmospheric transport is re-gridded from BETR-Research.[38] The finest resolution in NEM is constrained by the resolution of freshwater transport.

### Compartmentalization

NEM includes compartments describing a two-layer atmosphere (representing the boundary layer and the free troposphere),[37] forest canopies (needleleaf and broadleaf), soils (forest soils, agricultural soils and uncultivated soils), permanent snow/ice, fresh water and freshwater sediment, as well as seawater and marine sediment (Fig. S1†). NEM additionally includes a seasonal sea ice cover, parameterized on basis of the SODA3 ocean reanalysis. Area fractions for terrestrial compartments are based on the land cover classification from IGBP at 0.5° resolution.[45] Some minor adjustments were necessary to align the IGBP database with the requirements of WaterGAP and SODA3. A marine sediment compartment is assumed to be present in all coastal grid cells with run-off into the sea, and for marine grid cells with a seawater depth less than 600 meters. NEM is also integrated with the ACC-Human bioaccumulation model.[46]

### Other environmental input parameters

Long-term monthly means of temperature in air at 2 meters above the surface, wind speed at 10 m and daily precipitation at 0.5° resolution were taken from ECWMF (European Centre for Medium-Range Weather Forecasts – www.ecwmf.int). The durations of dry and wet periods were also calculated with data from ECWMF. Soil organic carbon content at 0.5° resolution was derived from global soil maps.[47,48] Monthly seawater temperatures and bathymetry were taken from SODA3.[44] The remaining environmental input parameters were adopted from CoZMoPOP2 (ref. 36) or BETR-Global.[38]

### Physical–chemical properties and emissions

For this initial study, we selected PCB-153 (2,2′,4,4′,5,5′-hexachlorobiphenyl) because (i) it is representative of the larger group of non-polar organic contaminants (ii) environmental and human exposure to PCBs remains high and toxicologically relevant[49,50] (iii) empirical data critical for model evaluation are plentiful, and (iv) a global historical emission inventory for PCBs is available.[51,52] Partition coefficients at 25 °C (octanol–water $K_{OW}$, octanol–air $K_{OA}$ and air–water $K_{AW}$) and energies of phase transfer for adjusting those coefficients to temperatures other than 25 °C were adopted from Li *et al.*[53] The rate constant for the gas-phase reaction of PCB-153 with OH radicals at 25 °C, along with the corresponding activation energy, were taken from Brubaker and Hites.[54] For reaction rates and activation energies in media other than air, we used the values by Wania and Su.[55] The most recent global historical emission inventory for PCB-153 was used to predict environmental concentrations (default scenario).[56] Reflecting the observed seasonal variability at a monitoring station influenced by local sources,[57] emissions are assumed to vary seasonally following a sine function with the warmest month in each grid cell having emissions 50% above the annual average.

### Model scenarios exploring impact of spatial resolution outside a nested European domain

It is well established that numerical diffusion in Eulerian box models with coarse resolution leads to overestimated concentrations in remote areas and underestimated concentrations in source regions.[58,59] Global HRTMs employ a fine spatial resolution to overcome this problem, but a fine spatial resolution may not necessarily be required on a global scale when the area of interest is a single confined region. Nevertheless, a coarse spatial resolution outside of a nested region could have an appreciable "edge effect" on model predictions within that region. The maximum number of grid cells in a single simulation in NEM is restricted to ~3000. The number of grid cells is constrained by the available memory within the software used. This limits the finest spatial resolution for a global simulation to 5°. To explore this edge-effect, we performed three global simulations at resolutions of 30°, 15° and 10°, each of which was followed by the simulation of a nested European domain (90°N, 30°W to 30°N, 30°E) at 5° (Fig. S2A†). We also included an additional simulation for the European domain at 5°, in which inflow of PCB-153 was set to zero (Fig. S2B†). The results obtained from a global simulation at 5° then served as the benchmark to which results from the four nested simulations were compared (Fig. S2C†).

### Model scenarios exploring impact of spatial resolution within a northern European domain

For model evaluation and application, we studied the impact of spatial resolution within northern Europe (85°N, 30°W to 45°N, 30°E) using three global simulations: non-nested with 15° resolution throughout; non-nested with 5° resolution throughout; and nested with 1° resolution in the nested northern European domain and 5° outside of it (Fig. 1 and S3†).

In all cases, simulations covered the years from 1930 to 2020 at time-steps of 6 hours (30°/15°), 3 hours (10°), 1 hour (5°) and 15 minutes (1°) with results stored six times per year.

### Monitoring data

The nested domain was chosen because of the relatively large number of long-term monitoring stations in northern Europe. We used monthly mean concentrations in background air from AMAP[19,60] and EMEP[18,61] (ebas.nilu.no) to evaluate the predicted

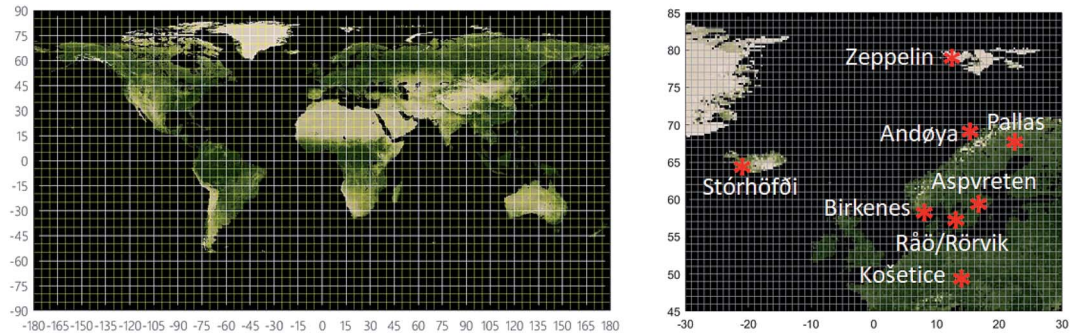


Fig. 1 The map on the left shows the global NEM model domains at the 15° and 5° resolutions. The map on the right shows the location of the air monitoring sites within the nested northern European domain at the 1° resolution.

spatial and temporal trends of PCB-153. The list of stations, station coordinates and years covered is included in Table S1.† The model evaluation is restricted to air because the focus of the model application is on LRAT.

### Visualizations

The Normalized Difference Vegetation Index (NDVI) image generated by NASA based on MODIS satellite observations was used for mapping results.

## Results and discussion

### Spatial resolution outside a nested domain

The advective chemical inflow *via* air, fresh water and seawater into a nested domain will depend on the emissions outside the nested domain as well as the spatial resolution selected for this external (to the nest) domain. Fig. S4† displays maps of the ratio of PCB-153 concentrations in air obtained for late summer 2015 from each of the nested simulations and those from the global benchmark simulation. If the global simulation was done at 30°, the predicted concentrations in the nested domain were higher than the benchmark simulation by factor of 1.96–1.26 over the entire year. When the global simulation was done at 15° and 10° resolution, that factor was reduced to 1.46–1.05 and 1.09–0.93, respectively. While predictions thus were still higher than in the global benchmark simulation, the increased spatial resolution outside the nested domain reduced the effect of numerical diffusion into the nested domain. Concentrations predicted with the scenario without advective inflow were always lower than in the benchmark simulation, although the difference relative to the benchmark simulation was minor (as low as 2%) in the major source region in central parts of Europe (*e.g.* UK, Germany and France)[51,52] (Fig. S3†).

Larger deviations were predicted for individual grid cells within the nested domain. The maximum ratios over the year were particularly large (up to 15.8) when relying on the coarsest resolution (30°) and declined with finer resolution (8.7 at 15°; 3.1 at 10°). The tendency to overpredict concentrations relative to the benchmark simulation was largest at the highest latitudes (Fig. S4†). For example, when the nested simulation relied on the finest outside resolution (10°), the average ratio over the year for the 5° grid cell in which the Zeppelin monitoring station on Svalbard is located was 1.23 (1.00–1.80).

There were also circumstances where predictions based on the global benchmark simulation exceeded predictions from any of the nested simulations, as seen over ocean areas near the western border of the domain (Fig. S4†). However, these minimum ratios were very similar for all of the nested simulations (0.36 at 30°, 0.33 at 15°, 0.36 at 10°). Such results may be anticipated when the global benchmark simulation resolves confined plumes extending outwards from source regions towards the boundaries of the nested domain (see also Fig. 4C). The ability to perform quantitative evaluations within a consistent modelling framework illustrates that this feature can be explored to inform tiered modelling strategies. While inflow into a nested domain from global sources will always be overestimated because of numerical diffusion outside the boundaries, the initial analysis shows that any "edge effect" as seen at the highest latitudes (Fig. S4†) can be greatly reduced by increasing the spatial resolution of the preceding domain (*e.g.* by further nesting).

### Model evaluation

Numerical diffusion can be further minimized by reducing the spatial resolution within the nested domain. Fig. 2 compares predicted and observed concentration time trends of PCB-153 in air at the nine monitoring sites with the longest time series at a spatial resolution down to 1° (Table S1,† results for four further sites with shorter time series are found in Fig. S5†). The extent of model-measurement agreement is further evaluated by comparing geometric means of observed and predicted concentrations for the period for which measurement data were available for each site (Fig. 3A). The geometric mean concentrations varied over more than an order of magnitude between sites, from 3.7 pg $m^{-3}$ at Košetice to 0.1 pg $m^{-3}$ at Andøya, and this range is largely captured by the model (Fig. 3A). The three model simulations predict a decline in concentrations at all sites (Fig. 2), consistent with the decline in primary emissions in the model domain over the time-period for which monitoring data are available. The predictions are broadly in line with temporal trends observed at most, but not all, of the sites. For example, a review of long-term temporal trends in Arctic air did

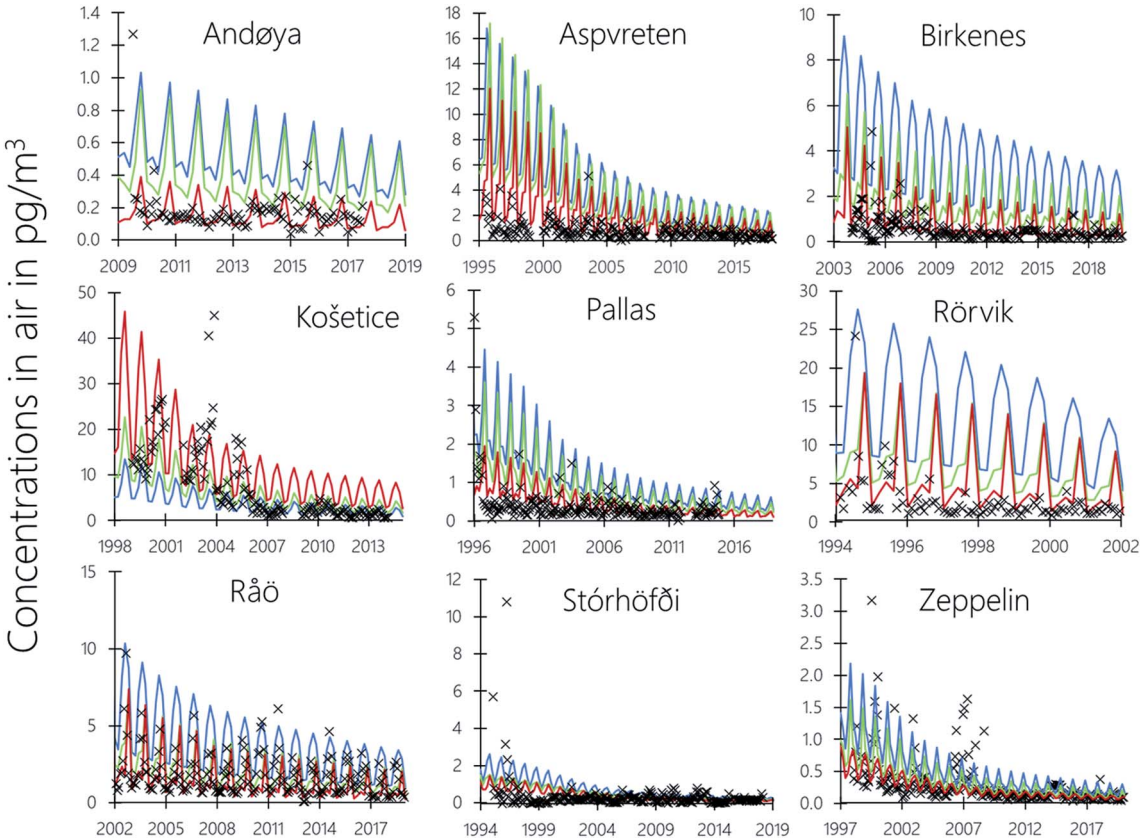


Fig. 2 Observed long-term trends of PCB-153 in air (black markers) and predictions with NEM at 15° (blue), 5° (green) and 1° (red) spatial resolution.

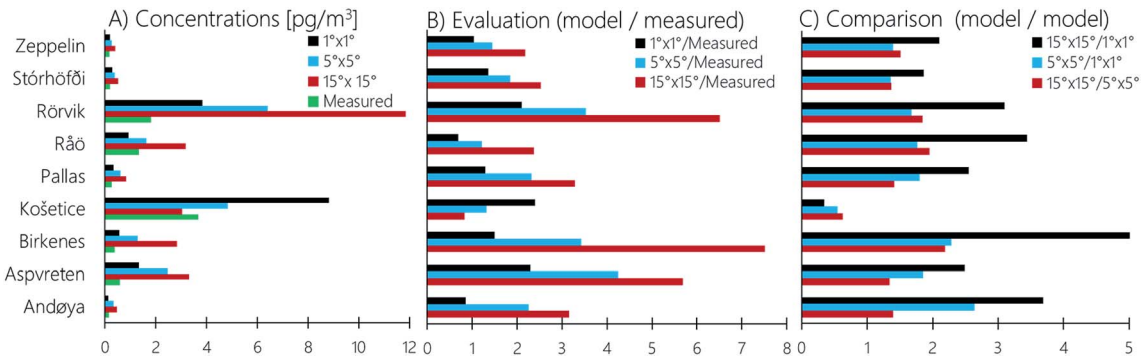


Fig. 3 Observed and predicted geometric mean concentrations (A), ratios between model predictions and measured concentrations (B) as well as ratios across model predictions (C) simulated using different resolutions. The predicted mean concentration is calculated from data for the grid cell in which the station is located for those years for which observed data are reported.

not identify any downward trend in concentrations of PCB-153 at Stórhöfði,[19] but NEM predicts such a decline.

The extent of agreement between predicted and observed temporal trends varies between sites (Fig. 2 and 3). This could be because sampling frequency and duration vary between sites. At the Swedish and Finnish stations weekly samples are collected throughout the year and analyzed in monthly pools,[62] which yields concentrations more directly comparable to the results of a model that relies on variables with a temporal resolution of a month. At Košetice, Stórhöfði, and the Norwegian sites air sampling is intermittent. For example, samples at Andøya were collected over 48 hours once per month in 2018. Such intermittently measured concentrations are subject to short-term fluctuations that cannot be captured by NEM. Some variability in model-measurement agreement between sites could also arise because they were generated in different laboratories. Differences of up to a factor two are plausible when trace amounts of PCBs are quantified in air samples.[63]

 

The extent of agreement between predicted and observed concentrations generally improved with increasing spatial resolution (Fig. 2 and 3). The predicted geometric mean concentration divided by the corresponding measured concentration at 15°, 5° and 1° across all nine sites was, on average, 3.8 (range: 0.8–7.5), 2.4 (range: 1.2–4.3) and 1.5 (range: 0.7–2.4), respectively (Fig. 3B). That these average ratios are larger than 1 implies that the model tended to overestimate observed concentrations of PCB-153 in air, irrespective of the spatial resolution. The tendency for better agreement with increasing spatial resolution was consistent for 7 out of 9 sites, with the notable exception of Košetice for reasons discussed below. There was a slightly better agreement for Råö at intermediate resolution compared to the finest resolution. Overall, the model evaluation shows that differences between observations when averaged over a month and model predictions at higher resolution are comparable to the variability anticipated from differences in sampling and analytical methods used across laboratories involved in the EMEP POPs programme.

### Comparison of model results at different resolution

NEM allows for a direct comparison of predictions obtained at different spatial resolution. Predictions at coarse resolution (15°) were 2–5 times higher than those at the finest resolution (1°) at all sites except Košetice (Fig. 3C). As the comparison of air concentrations at different resolution in Fig. 3C is restricted to grid cells containing monitoring stations, Fig. 4 displays maps with concentrations predicted with NEM, exemplified for late summer 2015, with three different resolutions as well as a map of the ratio between predictions obtained at the coarsest and the finest resolution. Similar plots for other points in time during 2015 are included in the ESI (Fig. S6–S8†). The three first panels in Fig. 4 highlight the effect of numerical diffusion on the predicted spatial dispersion of PCB-153. Concentrations in the northwestern part of the domain are clearly elevated at coarse resolution, whereas at fine resolution higher concentrations are predicted in central Europe in the southeastern part of the model domain, comprising the major PCB source regions (Fig. S3†).

The maps in Fig. 4 suggest that a coarse resolution overpredicts atmospheric dispersion and thereby overestimates concentrations in air across much of the domain. Concentrations predicted at 15° resolution were, on average, 3.4 times higher than those at 1° (Fig. 4), with the factor varying from 2.2 to 3.4 over the year (Fig. S9†). The difference between predictions obtained at 5° *versus* 1° was less pronounced, varying by a factor between 1.5 and 1.8 during 2015 (Fig. S10†).

In sharp contrast to most of the model domain, concentrations predicted for the southeastern PCB source regions at the 1° resolution were much higher than predictions at 15°. This is also a result of overestimated atmospheric dispersion from major source regions at coarse resolution. Košetice is the only sampling site that falls into that part of the model domain, which explains why it is also the only one where an increasing spatial resolution does not improve model-measurement agreement (Fig. 3B). The apparent better model-measurement agreement for Košetice at coarse resolution (Fig. 2 and 3B) may suggest that emissions affecting the 1° grid cells containing Košetice are overestimated. We attribute this to uncertainties in the emissions inventory which spatially distributes national emissions using population densities. While this might be a fair

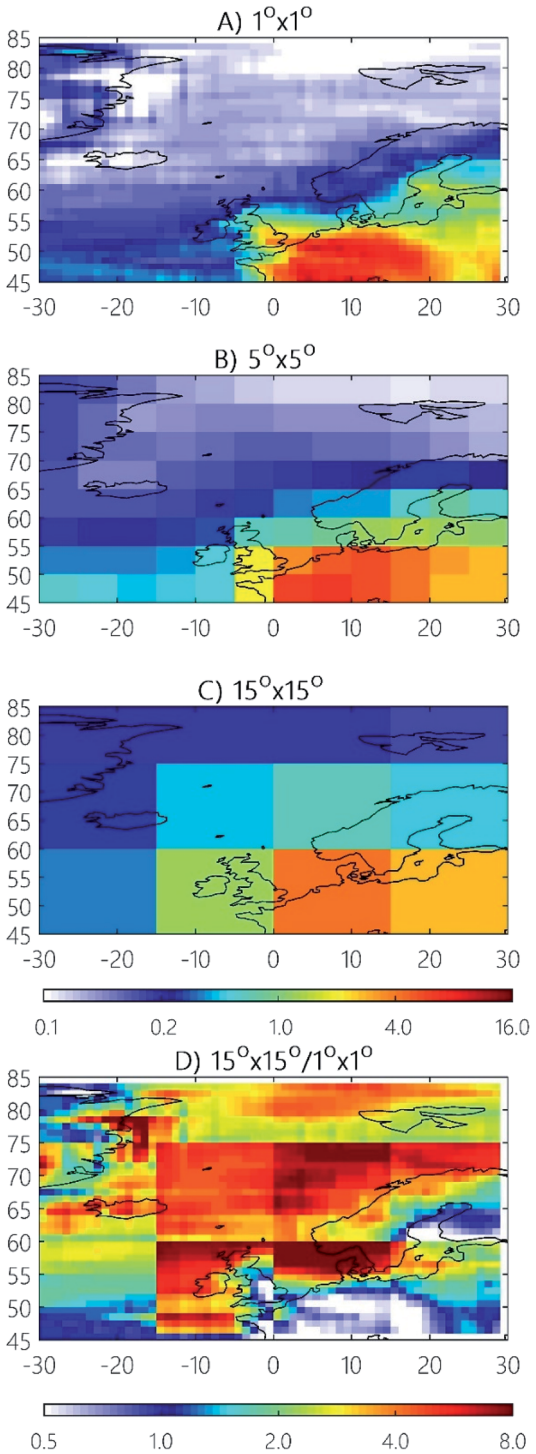


Fig. 4 Predicted concentrations of PCB-153 in air (pg $m^{-3}$) during late summer 2015 using NEM with different spatial resolutions (upper three panels). The lower panel shows the ratio of the concentrations predicted at a resolution of 15° and 1°.

approximation for models operating at a coarse resolution, it becomes increasingly unrealistic at finer spatial scales, *e.g.* because facilities treating PCB-containing waste are not necessarily located in the most densely populated areas of a nation. This suggests that the ability of the model to resolve spatial variability in concentrations in or close to PCB source regions is constrained by the accuracy of the emission inventory at finer resolution.[52] Furthermore, an accurate description of atmospheric dispersion becomes increasingly important when a station is located close to an area with strong emissions.

Fig. 4 also helps to explain the tendency towards better agreement with increasing spatial resolution, especially if the emissions inventory at 1° reveals a high spatial variability in emission strength within a 15° cell (Fig. S3†). A notable example is the 15° grid cell containing Birkenes in southern Norway (Fig. 1), for which predictions exceeded measurements by almost a factor of 8 (Fig. 2 and 3). This is because the same 15° grid cell also comprises major source regions in Central Europe. Simulations at higher resolution result in stronger modeled concentration gradients within that 15° cell (Fig. 4, lower panel). The map in Fig. 4 (lower panel) helps to identify regions where increasing spatial resolution is expected to be particularly important. These are regions with steep concentration gradients. Reducing model resolution reduces concentration gradients by two mechanisms: averaging out gradients within a cell, and flattening out gradients between cells (Fig. S9 and S10†).

### Applying NEM to compare inflow *versus* in-cell emissions

It is of interest to assess whether atmospheric burdens within a certain region are mainly controlled by atmospheric inflow from the outside or primarily dictated by emissions within the region. The ratio of these two flows is a measure of the remoteness of the location from sources, assessed on the scale of the grid cell. Whether this grid cell is remote or not will therefore depend on the resolution of the model. How to choose suitable measurement sites has been a topic within EMEP for many decades, dating back to assessments of LRAT for acidifying pollutants.[18,64] EMEP aims to sample at background sites where the air and precipitation quality parameters are representative of a larger region.[18,65] Since an important objective of monitoring in EMEP is also to evaluate atmospheric transport models, the size of the area a site is expected to represent has historically been constrained by the spatial resolution of early EMEP models. Compared to air pollutants that are more easily measured, monitoring sites for POPs are very limited in number (Fig. 1).[18] We therefore applied NEM to assess how representative a site is in terms of remoteness within the area (grid cell) in which they are located.

We calculated the fraction of the total PCB-153 input to a grid cell that is originating from outside this cell, *i.e.* is not attributed to local emissions within that cell. We caution that this measure assumes that any molecule which were initially emitted in a grid cell never returns. This calculation was done for the grid cells containing air monitoring sites and for different spatial resolution (Fig. 5). If a site is located within a cell without emissions, atmospheric inflow is the only source

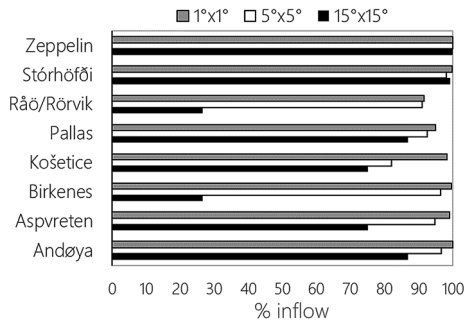


Fig. 5 Relative significance of atmospheric inflow to the sum of atmospheric inflow plus emissions for grid cells in which a monitoring station is located, simulated using three different spatial resolutions, 1930–2020.

of PCB-153. This is the case for Zeppelin, irrespective of the spatial resolution, as well as for Andøya at 1°. For most sites and resolutions, inflow from the outside dominates, making a contribution of more than 75% (Fig. 5). The notable exception was the 15° grid cell containing Birkenes and Råö/Rörvik, where only ~27% of the PCB-153 is estimated to originate from outside. This occurs because this cell comprises areas with high emissions in central Europe as well as parts with comparatively low emissions, including the regions where Birkenes and Råö/Rörvik are located (Fig. 4 and S3†). This leads to a high estimated contribution from local emissions at coarse resolution, which is not representative of the actual situation at those sites. At increasing resolution, these and many other sites become increasingly influenced by atmospheric inflow. At 1°, atmospheric inflow is predicted to contribute close to 100% of PCB-153 to the cell containing Birkenes, and ~92% to that containing Räø/Rörvik. The general pattern of decreasing influence of local emissions with increasing resolution indicates that the sites are generally remote within the larger region in which they are located. The exception is Stórhöfði where local sources make the highest contribution at a resolution of 5°. This is because at that resolution Stórhöfði shares a cell with Reykjavik (61°14′N, 21°94′E), where most of the Icelandic PCB emissions are assumed to occur, but at a 1° resolution they are in separate cells. At a resolution of 15° (Fig. 4), Icelandic emissions become negligible when distributed within a very large grid cell. A similar situation to Stórhöfði is evident for High Muffles (coastal site in N. England) and Westerland (west coast of Germany, close to the Danish border) which both are seen as remote at a resolution of 1°, but not 5° (Fig. S5†).

A numerical threshold is required to define a grid cell as remote or not. If an (arbitrary) cut-off of less than 95% is chosen, then the cells containing Stórhöfði and Zeppelin will be defined as remote at all model resolutions. The cells containing Andøya and Birkenes are remote at 5°, Aspvreten and Košetice at 1°, while Pallas falls just below this threshold at 1° (94.9%). The cell containing Räø/Rörvik which always includes Göteborg, the second largest city in Sweden, is not defined as remote at any spatial resolution (91.5 at 1°). To what extent a grid cell containing a specific background monitoring station is remote

therefore depends on the model resolution, while a threshold is required to identify whether the cell is remote or not. If the site is close to source regions, the desirable spatial resolution is likely to be higher and will depend on the grid cell's source proximity.

The simple approach used herein, calculating emissions *vs.* inflow to assess whether and to what extent a site monitors LRAT, resembles attempts to establish measures of remoteness using generic emission scenarios *e.g.*[38] If realistic emission scenarios are available, NEM can help to plan where to collect air samples.[14,66] Fig. S11† shows results across the model domain at 15°, 5° and 1°. Applying the cut-off at 95% for model predictions at 15°, 7 out of 16 grid cells will qualify as remote. The two adjacent grid cells which include the UK (60°N, 15°W to 45°N, 0°E) and Germany/France (60°N, 15°W to 45°N, 0°E) are predicted to be predominantly controlled by emissions within these grid cells. The percentage inflows are predicted to be 41.9% and 26.6% respectively. Räø/Rörvik and Birkenes fall into the latter grid cell (Fig. 5). At a resolution of 5°, 34 grid cells qualify as remote. Two out of the 108 grid cells in total are predicted to be mainly controlled by emissions, rather than inflow. These two cells cover central parts of England (55°N, 5°W to 50°N, 5°W) and central parts of France (50°N, 0°W to 45°N, 5°E) with predicted inflows of 33.2% and 48.3%, respectively. At a resolution of 1°, emissions occur in 666 out of 2400 grid cells in total whereby 463 grid cells classify as remote. Only a single grid cell (London) is predicted to be predominantly influenced by local emissions (48.8% inflow) at 1° resolution. The results presented in Fig. S11† summarize how numerical diffusion both leads to overestimated atmospheric dispersion from major source regions and LRAT into remote northern sites.

### Applying NEM to resolve spatial gradients in atmospheric deposition to the Baltic Sea

The occurrence of PCBs in the Baltic Sea has been extensively studied for more than half a century, *e.g.*67,68 Previous studies have highlighted the role of atmospheric deposition and air–sea exchange in controlling the levels and fate of PCBs in the Baltic Sea. *e.g.*[69–71] A review of temporal trends of PCBs in biota over ~30 years across the Baltic Sea suggested that airborne transport has been the key factor controlling contaminant burdens in the Baltic Sea, with local and regional sources and LRAT all having played a role.[72] It follows that accurate quantification of atmospheric input is crucial for understanding the fate of PCBs in the Baltic Sea. Because this body of water extends from PCB source regions in the Southwest to more remote regions in the North, predictions of atmospheric inputs are likely to depend strongly on spatial resolution. We have therefore compared the atmospheric deposition of PCB-153 to the Baltic Sea in 2015, when calculated with NEM at resolutions of 1°, 5° and 15° (Fig. S12–S14†). The atmospheric deposition predicted at 15° generally exceeded predictions at the finest resolution by a factor of about ~2 (1.5–2.2) for the Baltic Sea as a whole during most of the year except for the late fall (0.7) (Table S2†). Differences are much more pronounced for individual sub-basins, with discrepancies in estimated deposition for the Bothnian Sea (defined as the Baltic Sea >60°N) during winter, and the Kattegat/Skagerrak region (<15°E) during summer, occasionally exceeding one order of magnitude for individual grid cells (Fig. S15†). This example highlights the significance of numerical diffusion for compartments other than air, and the need for fine resolution when targeting specific receiving environments of interest.

## Conclusions

The NEM model allows for both targeting and integrating regional, continental and global scales through nesting. The effect of numerical diffusion has been explored by varying the spatial resolution selected outside of a nested European region simulated at 5°. This "edge effect" was found to be most pronounced for grid cells at the boundaries of the highest latitude, but it was greatly reduced by increasing the spatial resolution outside the nested domain from 30° to 10°. The evaluation for the nested northern European model domain, simulated at 1°, demonstrated a very good agreement with concentrations of PCB-153 in air measured at nine long-term monitoring sites. While there was a slight tendency to overestimate observed concentrations in air, the deviations between predictions are comparable to the variability expected from differences in sampling and analytical methods alone. The model predicted that ~92% or more of the atmospheric burden within the grid cells containing an EMEP site can be attributed to advective atmospheric transport from outside those cells at a resolution of 1°. However, the ability of the model to resolve spatial variability in concentrations within or adjacent to PCB source regions becomes increasingly constrained by the accuracy of the emission inventory at finer resolution.

An advantage of NEM is the ability to flexibly select spatial resolutions and nesting strategies in a way that matches the resolution of the emission inventory, rather than operating HRTMs on the basis of emissions data that are more coarsely resolved than the model. The latter approach may lead to an overparameterization with respect to the available emission inventory. For some countries and regions more highly spatially resolved emission inventories[73,74] may be available than what is available at coarser scales (*e.g.* globally). Under such circumstances, NEM allows for a harmonized nesting strategy which matches the model resolution to the available emission inventories at various scales.

An obvious advantage of a nested modelling strategy is that its computational efficiency allows for simulations of large number of substances (*e.g.* complex mixtures or groups of chemicals). Multimedia models have been shown to be suitable for simulating the fate of complex compound mixtures based on defining input parameters for blocks of closely related substances, *e.g.* hydrocarbon mixtures in gasoline[75,76] or different formula groups of the short-chain chlorinated paraffins.[40] However, while previous efforts of this type were restricted to relatively simple non-spatially resolved models, NEM opens up the possibility to simulate spatial and temporal aspects of the fate of contaminant mixtures, *e.g.* by investigating

how mixture composition will change in space and time. This is feasible because a nested approach allows for spatially resolved, dynamic simulations of dozens of mixture components with reasonable computational resources. It should also be feasible to screen large numbers of chemicals for LRAT with a NEM-based approach, when spatial variability in LRAT is an important aspect of the assessment.[77–79]

The scope of testing and applying the model in this study was restricted to PCB-153 in air within northern Europe. There clearly is a need for future efforts to test the model for other regions, contaminants and compartments to help identify areas for further improvements as well as to characterize the domain of applicability. However, the flexible model geometries and resolutions make us optimistic that NEM will prove useful in future studies of scientific and/or regulatory interest. The choice of resolution will depend on the purpose and requirements of a model simulation as illustrated for the Baltic Sea. Ideally, a simulation using NEM should be done at the finest resolution achievable with the available computing resources (*i.e.* model and CPU time). As those resources will always be restricted, NEM offers a rationale for targeting most of the limited resources towards those aspects of a model simulation which are of greatest interest.

## Conflicts of interest

There are no conflicts to declare.

## Author contributions

Knut Breivik: conceptualization, data curation, formal analysis, funding acquisition, investigation, methodology, project administration, resources, software, validation, visualization, writing – original draft. Sabine Eckhardt: conceptualization, data curation, formal analysis, investigation, methodology, software, visualization, writing – review & editing. Michael S. McLachlan: conceptualization, funding acquisition, supervision, methodology, writing – review & editing. Frank Wania: conceptualization, funding acquisition, supervision, methodology, writing – review & editing.

## Acknowledgements

We would like to thank Matt MacLeod and Fangyuan Zhao for providing high resolution data from BETR-Global, the US Geological Survey for providing the IGBP inventory through Global Land Cover Characteristics Data Base Version 2.0, Tim Trautmann (Goethe Universität, Germany) for providing data on fresh water flows and directions, and Matt MacLeod, Wenche Aas and Ingjerd S. Krogseth for helpful discussions. We further acknowledge the continuous efforts by all scientists and staff involved in the EMEP POPs monitoring programme. The study was financed by the Norwegian Research Council (#244298) and the Long-range Research Initiative of the European Chemical Industry Council (project ECO-53).

## References

1 UNEP, *The Stockholm Convention on Persistent Organic Pollutants (POPs)*.
2 UNECE, *The 1998 Aarhus Protocol on POPs*, www.unece.org/env/lrtap/pops_h1.htm.
3 AMAP, Trends in Stockholm Convention Persistent Organic Pollutants (POPs) in Arctic Air, Human media and Biota, *Arctic Monitoring and Assessment Programme, Technical Report no 7*, ISBN 978-82-7971-084-4, 2014.
4 B. Ottar, The transfer of airborne pollutants to the Arctic region, *Atmos. Environ.*, 1981, **15**(8), 1439–1445, DOI: 10.1016/0004-6981(81)90350-4.
5 H. Hung, P. Blanchard, C. J. Halsall, T. F. Bidleman, G. A. Stern, P. Fellin, D. C. G. Muir, L. A. Barrie, L. M. Jantunen, P. A. Helm, J. Ma and A. Konoplev, Temporal and spatial variabilities of atmospheric polychlorinated biphenyls (PCBs), organochlorine (OC) pesticides and polycyclic aromatic hydrocarbons (PAHs) in the Canadian Arctic: Results from a decade of monitoring, *Sci. Total Environ.*, 2005, **342**(1–3), 119–144, DOI: 10.1016/j.scitotenv.2004.12.058.
6 R. Kallenborn, M. Oehme, D. D. Wynn-Williams, M. Schlabach and J. Harris, Ambient air levels and atmospheric long-range transport of persistent organochlorines to Signy Island, Antarctica, *Sci. Total Environ.*, 1998, **220**(2–3), 167–180, DOI: 10.1016/S0048-9697(98)00257-5.
7 K. Pozo, T. Harner, M. Shoeib, R. Urrutia, R. Barra, O. Parra and S. Focardi, Passive-sampler derived air concentrations of persistent organic pollutants on a north-south transect in Chile, *Environ. Sci. Technol.*, 2004, **38**(24), 6529–6537, DOI: 10.1021/es049065i.
8 J. Kalina, M. Scheringer, J. Boruvkova, P. Kukucka, P. Pribylova, O. Sanka, L. Melymuk, M. Vana and J. Klanova, Characterizing Spatial Diversity of Passive Sampling Sites for Measuring Levels and Trends of Semivolatile Organic Chemicals, *Environ. Sci. Technol.*, 2018, **52**(18), 10599–10608, DOI: 10.1021/acs.est.8b03414.
9 Z. Zhang, L. Y. Liu, Y. F. Li, D. G. Wang, H. L. Jia, T. Harner, E. Sverko, X. N. Wan, D. D. Xu, N. Q. Ren, J. M. Ma and K. Pozo, Analysis of polychlorinated biphenyls in concurrently sampled Chinese air and surface soil, *Environ. Sci. Technol.*, 2008, **42**(17), 6514–6518, DOI: 10.1021/es8004078.
10 W. A. Ockenden, A. J. Sweetman, H. F. Prest, E. Steinnes and K. C. Jones, Toward an understanding of the global atmospheric distribution of persistent organic pollutants: The use of semipermeable membrane devices as time-integrated passive samplers, *Environ. Sci. Technol.*, 1998, **32**(18), 2795–2803, DOI: 10.1021/es9802145.
11 S. N. Meijer, E. Steinnes, W. A. Ockenden and K. C. Jones, Influence of environmental variables on the spatial distribution of PCBs in Norwegian and UK soils: Implications for global cycling, *Environ. Sci. Technol.*, 2002, **36**(10), 2146–2153, DOI: 10.1021/es010322i.

 

12 L. Shen, F. Wania, Y. D. Lei, C. Teixeira, D. C. G. Muir and H. Xiao, Polychlorinated biphenyls and polybrominated diphenyl ethers in the North American atmosphere, *Environ. Pollut.*, 2006, **144**(2), 434–444, DOI: 10.1016/j.envpol.2005.12.054.

13 J. Klanova, P. Cupr, I. Holoubek, J. Boruvkova, P. Pribylova, R. Kares, T. Tomsej and T. Ocelka, Monitoring of persistent organic pollutants in Africa. Part 1: Passive air sampling across the continent in 2008, *J. Environ. Monit.*, 2009, **11**(11), 1952–1963, DOI: 10.1039/b913415h.

14 F. M. Jaward, N. J. Farrar, T. Harner, A. J. Sweetman and K. C. Jones, Passive air sampling of PCBs, PBDEs, and organochlorine pesticides across Europe, *Environ. Sci. Technol.*, 2004, **38**(1), 34–41, DOI: 10.1021/es034705n.

15 T. M. Jaward, G. Zhang, J. J. Nam, A. J. Sweetman, J. P. Obbard, Y. Kobara and K. C. Jones, Passive air sampling of polychlorinated biphenyls, organochlorine compounds, and polybrominated diphenyl ethers across Asia, *Environ. Sci. Technol.*, 2005, **39**(22), 8638–8645, DOI: 10.1021/es051382h.

16 K. Pozo, T. Harner, F. Wania, D. C. G. Muir, K. C. Jones and L. A. Barrie, Toward a global network for persistent organic pollutants in air: Results from the GAPS study, *Environ. Sci. Technol.*, 2006, **40**(16), 4867–4873, DOI: 10.1021/es060447t.

17 H. Hung, M. MacLeod, R. Guardans, M. Scheringer, R. Barra, T. Hamer and G. Zhang, Toward the next generation of air quality monitoring: Persistent organic pollutants, *Atmos. Environ.*, 2013, **80**, 591–598, DOI: 10.1016/j.atmosenv.2013.05.067.

18 K. Tørseth, W. Aas, K. Breivik, A. M. Fjaeraa, M. Fiebig, A. G. Hjellbrekke, C. L. Myhre, S. Solberg and K. E. Yttri, Introduction to the European Monitoring and Evaluation Programme (EMEP) and observed atmospheric composition change during 1972-2009, *Atmos. Chem. Phys.*, 2012, **12**(12), 5447–5481, DOI: 10.5194/acp-12-5447-2012.

19 H. Hung, A. A. Katsoyiannis, E. Brorström-Lundén, K. Olafsdottir, W. Aas, K. Breivik, P. Bohlin-Nizzetto, A. Sigurdsson, H. Hakola, R. Bossi, H. Skov, E. Sverko, E. Barresi, P. Fellin and S. Wilson, Temporal trends of Persistent Organic Pollutants (POPs) in arctic air: 20 years of monitoring under the Arctic Monitoring and Assessment Programme (AMAP), *Environ. Pollut.*, 2016, **217**, 52–61, DOI: 10.1016/j.envpol.2016.01.079.

20 B. R. Hillery, M. F. Simcik, I. Basu, R. M. Hoff, W. M. J. Strachan, D. Burniston, C. H. Chan, K. A. Brice, C. W. Sweet and R. A. Hites, Atmospheric deposition of toxic pollutants to the Great Lakes as measured by the integrated atmospheric deposition network, *Environ. Sci. Technol.*, 1998, **32**(15), 2216–2221, DOI: 10.1021/es970759j.

21 UNEP, *Guidance on the global monitoring plan for persistent organic pollutants, Stockholm Convention on Persistent Organic Pollutants, UNEP/POPS/COP.7/INF/39*, http://www.pops.int/Portals/0/download.aspx?d=UNEP-POPS-COP.7-INF-39.English.pdf.

22 UNEP, *Second Global Monitoring Report. Global Monitoring Plan for Persistent Organic Pollutants under the Stockholm Convention Article 16 on Effectiveness Evaluation, UNEP/POPS/COP.8/INF/38*, 2017.

23 D. Woodfine, M. MacLeod and D. Mackay, A regionally segmented national scale multimedia contaminant fate model for Canada with GIS data input and display, *Environ. Pollut.*, 2002, **119**(3), 341–355, DOI: 10.1016/S0269-7491(01)00344-X.

24 K. Kawamoto, M. MacLeod and D. Mackay, Evaluation and comparison of multimedia mass balance models of chemical fate: application of EUSES and ChemCAN to 68 chemicals in Japan, *Chemosphere*, 2001, **44**(4), 599–612, DOI: 10.1016/S0045-6535(00)00348-9.

25 M. Margni, D. W. Pennington, C. Amman and O. Jolliet, Evaluating multimedia/multipathway model intake fraction estimates using POP emission and monitoring data, *Environ. Pollut.*, 2004, **128**(1–2), 263–277, DOI: 10.1016/j.envpol.2003.08.036.

26 D. G. Woodfine, M. MacLeod, D. Mackay and J. R. Brimacombe, Development of continental scale multimedia contaminant fate models: Integrating GIS, *Environ. Sci. Pollut. Res.*, 2001, **8**(3), 164–172, DOI: 10.1007/BF02987380.

27 M. MacLeod, D. G. Woodfine, D. Mackay, T. McKone, D. Bennett and R. Maddalena, BETR North America: A regionally segmented multimedia contaminant fate model for North America, *Environ. Sci. Pollut. Res.*, 2001, **8**(3), 156–163.

28 K. Prevedouros, M. MacLeod, K. C. Jones and A. J. Sweetman, Modelling the fate of persistent organic pollutants in Europe: parameterisation of a gridded distribution model, *Environ. Pollut.*, 2004, **128**(1–2), 251–261, DOI: 10.1016/j.envpol.2003.08.041.

29 K. Breivik and F. Wania, Mass budgets, pathways, and equilibrium states of two hexachlorocyclohexanes in the Baltic Sea environment, *Environ. Sci. Technol.*, 2002, **36**(5), 1024–1032, DOI: 10.1021/es001972+.

30 M. Scheringer, Persistence and spatial range as endpoints of an exposure-based assessment of organic chemicals, *Environ. Sci. Technol.*, 1996, **30**(5), 1652–1659, DOI: 10.1021/es9506418.

31 M. Macleod, W. J. Riley and T. E. McKone, Assessing the influence of climate variability on atmospheric concentrations of polychlorinated biphenyls using a global-scale mass balance model (BETR-global), *Environ. Sci. Technol.*, 2005, **39**(17), 6749–6756, DOI: 10.1021/es048426r.

32 S. Semeena and G. Lammel, Effects of various scenarios of entry of DDT and gamma-HCH on the global environmental fate as predicted by a multicompartment chemistry-transport model, *Fresenius Environ. Bull.*, 2003, **12**(8), 925–939.

33 S. L. Gong, P. Huang, T. L. Zhao, L. Sahsuvar, L. A. Barrie, J. W. Kaminski, Y. F. Li and T. Niu, GEM/POPs: a global 3-D dynamic model for semi-volatile persistent organic pollutants - Part 1: Model description and evaluations of air concentrations, *Atmos. Chem. Phys.*, 2007, **7**(15), 4001–4013, DOI: 10.5194/acp-7-4001-2007.

34 C. L. Friedman and N. E. Selin, Long-Range Atmospheric Transport of Polycyclic Aromatic Hydrocarbons: A Global 3-D Model Analysis Including Evaluation of Arctic Sources, *Environ. Sci. Technol.*, 2012, **46**(17), 9501–9510, DOI: 10.1021/es301904d.

35 A. K. Halse, S. Eckhardt, M. Schlabach, A. Stohl and K. Breivik, Forecasting long-range atmospheric transport episodes of polychlorinated biphenyls using FLEXPART, *Atmos. Environ.*, 2013, **71**, 335–339, DOI: 10.1016/j.atmosenv.2013.02.022.

36 F. Wania, K. Breivik, N. J. Persson and M. S. McLachlan, CoZMo-POP 2 - A fugacity-based dynamic multi-compartmental mass balance model of the fate of persistent organic pollutants, *Environ. Model. Software*, 2006, **21**(6), 868–884, DOI: 10.1016/j.envsoft.2005.04.003.

37 M. MacLeod, H. von Waldow, P. Tay, J. M. Armitage, H. Wohrnschimmel, W. J. Riley, T. E. McKone and K. Hungerbuhler, BETR global - A geographically-explicit global-scale multimedia contaminant fate model, *Environ. Pollut.*, 2011, **159**(5), 1442–1445, DOI: 10.1016/j.envpol.2011.01.038.

38 R. K. Göktas and M. MacLeod, Remoteness from sources of persistent organic pollutants in the multi-media global environment, *Environ. Pollut.*, 2016, **217**, 33–41, DOI: 10.1016/j.envpol.2015.12.058.

39 K. Breivik, G. Czub, M. S. McLachlan and F. Wania, Towards an understanding of the link between environmental emissions and human body burdens of PCBs using CoZMoMAN, *Environ. Int.*, 2010, **36**(1), 85–91, DOI: 10.1016/j.envint.2009.10.006.

40 I. S. Krogseth, K. Breivik, J. A. Arnot, F. Wania, A. R. Borgen and M. Schlabach, Evaluating the environmental fate of short-chain chlorinated paraffins (SCCPs) in the Nordic environment using a dynamic multimedia model, *Environ. Sci.: Processes Impacts*, 2013, **15**(12), 2240–2251, DOI: 10.1039/c3em00407d.

41 K. Breivik, M. McLeod, F. Wania and S. Eckhardt, Towards a nested exposure model for organic contaminants (NEM), *Organohalogen Compd.*, 2017, **79**, 516–520.

42 H. Muller Schmied, S. Eisner, D. Franz, M. Wattenbach, F. T. Portmann, M. Florke and P. Doll, Sensitivity of simulated global-scale freshwater fluxes and storages to input data, hydrological model structure, human water use and calibration, *Hydrol. Earth Syst. Sci.*, 2014, **18**(9), 3511–3538, DOI: 10.5194/hess-18-3511-2014.

43 P. Döll and B. Lehner, Validation of a new global 30-min drainage direction map, *J. Hydrol.*, 2002, **258**(1–4), 214–231, DOI: 10.1016/s0022-1694(01)00565-0.

44 J. A. Carton, G. A. Chepurin and L. G. Chen, SODA3: A New Ocean Climate Reanalysis, *J. Clim.*, 2018, **31**(17), 6967–6983, DOI: 10.1175/jcli-d-18-0149.1.

45 A. S. Belward, *The IGBP-DIS global 1 km land cover data set: proposal and implementation plans: report of the Land Recover Working Group of IGBP-DIS*, IGBP-DIS, Toulouse, 1996.

46 G. Czub and M. S. McLachlan, A food chain model to predict the levels of lipophilic organic contaminants in humans, *Environ. Toxicol. Chem.*, 2004, **23**(10), 2356–2366, DOI: 10.1897/03-317.

47 FAO, *Soil map of the world 1:5000000*, 1974, vol. 1.

48 N. Batjes, *ISRIC-WISE global data set of derived soil properties on a 0.5 by 0.5 degreed grid (Version 3.0). Report 2005/08*, ISRIC- World Soil Information, Wageningen, (with data set), 2005.

49 J. A. Arnot, J. M. Armitage, L. S. McCarty, F. Wania, I. T. Cousins and L. Toose-Reid, Toward a Consistent Evaluative Framework for POP Risk Characterization, *Environ. Sci. Technol.*, 2011, **45**(1), 97–103, DOI: 10.1021/es102551d.

50 EFSA Panel on Contaminants in the Food Chain, Scientific Opinion on the risk for animal and human health related to the presence of dioxins and dioxin-like PCBs in feed and food, *EFSA J.*, 2018, **16**, 331, DOI: 10.2903/j.efsa.2018.5333.

51 K. Breivik, A. Sweetman, J. M. Pacyna and K. C. Jones, Towards a global historical emission inventory for selected PCB congeners - a mass balance approach 1 Global production and consumption, *Sci. Total Environ.*, 2002, **290**(1–3), 181–198, DOI: 10.1016/S0048-9697(01)01075-0.

52 K. Breivik, A. Sweetman, J. M. Pacyna and K. C. Jones, Towards a global historical emission inventory for selected PCB congeners - a mass balance approach 2 Emissions, *Sci. Total Environ.*, 2002, **290**(1–3), 199–224, DOI: 10.1016/S0048-9697(01)01076-2.

53 N. Q. Li, F. Wania, Y. D. Lei and G. L. Daly, A comprehensive and critical compilation, evaluation, and selection of physical-chemical property data for selected polychlorinated biphenyls, *J. Phys. Chem. Ref. Data*, 2003, **32**(4), 1545–1590, DOI: 10.1063/1.1562632.

54 W. W. Brubaker and R. A. Hites, Gas phase oxidation products of biphenyl and polychlorinated biphenyls, *Environ. Sci. Technol.*, 1998, **32**(24), 3913–3918, DOI: 10.1021/es9805021.

55 F. Wania and Y. S. Su, Quantifying the global fractionation of polychlorinated biphenyls, *Ambio*, 2004, **33**(3), 161–168.

56 K. Breivik, J. M. Armitage, F. Wania, A. J. Sweetman and K. C. Jones, Tracking the Global Distribution of Persistent Organic Pollutants Accounting for E-Waste Exports to Developing Regions, *Environ. Sci. Technol.*, 2016, **50**(2), 798–805, DOI: 10.1021/acs.est.5b04226.

57 J. E. Haugen, F. Wania and Y. D. Lei, Polychlorinated biphenyls in the atmosphere of southern Norway, *Environ. Sci. Technol.*, 1999, **33**(14), 2340–2345, DOI: 10.1021/es9812397.

58 C. S. Warren, D. Mackay, E. Webster and J. A. Arnot, A cautionary note on implications of the well-mixed compartment assumption as applied to mass balance models of chemical fate in flowing systems, *Environ. Toxicol. Chem.*, 2009, **28**(9), 1858–1865, DOI: 10.1897/08-569.1.

59 Y. Rastigejev, R. Park, M. P. Brenner and D. J. Jacob, Resolving intercontinental pollution plumes in global models of atmospheric transport, *J. Geophys. Res.: Atmos.*, 2010, **115**, DOI: 10.1029/2009jd012568.

60 AMAP, *AMAP/Arctic Monitoring & Assessment Programme*, www.amap.no(14.09.20).
61 EMEP, *EMEP, Co-operative programme for monitoring and evaluation of the long-range transmission of air pollutants in Europe*, https://www.emep.int/(16.09.20).
62 W. Aas and P. Bohlin-Nizzetto, *Heavy metals and POP measurements, EMEP/CCC Report 3/2020 2020*, 2018.
63 Y. S. Su and H. L. Hung, Inter-laboratory comparison study on measuring semi-volatile organic chemicals in standards and air samples, *Environ. Pollut.*, 2010, **158**(11), 3365–3371, DOI: 10.1016/j.envpol.2010.07.041.
64 T. Berg and J. Schaug, *EMEP Workshop on the Accuracy of Measurements with WMO-sponsored sessions on Determining the Representativeness of Measured Parameters in a Given Grid Square as Compared to Model Calculations, EMEP/CCC-Report 2/1994*, 1994.
65 S. Henne, D. Brunner, D. Folini, S. Solberg, J. Klausen and B. Buchmann, Assessment of parameters describing representativeness of air quality in situ measurement sites, *Atmos. Chem. Phys.*, 2010, **10**(8), 3561–3581, DOI: 10.5194/acp-10-3561-2010.
66 F. M. Jaward, N. J. Farrar, T. Harner, A. J. Sweetman and K. C. Jones, Passive air sampling of polycyclic aromatic hydrocarbons and polychlorinated naphthalenes across Europe, *Environ. Toxicol. Chem.*, 2004, **23**(6), 1355–1364, DOI: 10.1897/03-420.
67 S. Jensen, A. G. Johnels, M. Olsson and G. Otterlind, DDT and PCB in marine animals from Swedish waters, *Nature*, 1969, **224**(5216), 247, DOI: 10.1038/224247a0.
68 E. Nyberg, S. Faxneld, S. Danielsson, U. Eriksson, A. Miller and A. Bignert, Temporal and spatial trends of PCBs, DDTs, HCHs, and HCB in Swedish marine biota 1969-2012, *Ambio*, 2015, **44**, S484–S497, DOI: 10.1007/s13280-015-0673-5.
69 C. Agrell, L. Okla, P. Larsson, C. Backe and F. Wania, Evidence of latitudinal fractionation of polychlorinated biphenyl congeners along the Baltic Sea region, *Environ. Sci. Technol.*, 1999, **33**(8), 1149–1156.
70 R. Bruhn, S. Lakaschus and M. S. McLachlan, Air/sea gas exchange of PCBs in the southern Baltic Sea, *Atmos. Environ.*, 2003, **37**(24), 3445–3454, DOI: 10.1016/s1352-2310(03)00329-7.
71 J. Axelman, D. Broman and C. Naf, Vertical flux and particulate/water dynamics of polychlorinated biphenyls (PCBs) in the open Baltic Sea, *Ambio*, 2000, **29**(4–5), 210–216.
72 A. Bignert, M. Olsson, W. Persson, S. Jensen, S. Zakrisson, K. Litzen, U. Eriksson, L. Haggberg and T. Alsberg, Temporal trends of organochlorines in Northern Europe, 1967-1995. Relation to global fractionation, leakage from sediments and international measures, *Environ. Pollut.*, 1998, **99**(2), 177–198.
73 J. Gluge, C. Steinlin, S. Schalles, L. Wegmann, J. Tremp, K. Breivik, K. Hungerbuhler and C. Bogdal, Import, use, and emissions of PCBs in Switzerland from 1930 to 2100, *PLoS One*, 2017, **12**(10), DOI: 10.1371/journal.pone.0183768.
74 O. Travnikov; N. Batrakova; A. Gusev; I. Ilyin; M. Kleimenov; O. Rozovskaya; V. Shatalov; I. Strijkina; W. Aas; K. Breivik; P. B. Nizzetto; K. Pfaffhuber; K. Mareckova; S. Poupa; R. Wankumueller and K. Seussall, *Assessment of transboundary pollution by toxic substances: Heavy metals and POPs, EMEP Status Report 2/2020*, 2020.
75 M. MacLeod, T. E. McKone, K. L. Foster, R. L. Maddalena, T. F. Parkerton and D. Mackay, Applications of contaminant fate and bioaccumulation models in assessing ecological risks of chemicals: A case study for gasoline hydrocarbons, *Environ. Sci. Technol.*, 2004, **38**(23), 6225–6233, DOI: 10.1021/es049752+.
76 K. L. Foster, D. MacKay, T. F. Parkerton, E. Webster and L. Milford, Five-stage environmental exposure assessment strategy for mixtures: Gasoline as a case study, *Environ. Sci. Technol.*, 2005, **39**(8), 2711–2718.
77 K. Fenner, M. Scheringer, M. MacLeod, M. Matthies, T. McKone, M. Stroebe, A. Beyer, M. Bonnell, A. C. Le Gall, J. Klasmeier, D. Mackay, D. Van De Meent, D. Pennington, B. Scharenberg, N. Suzuki and F. Wania, Comparing estimates of persistence and long-range transport potential among multimedia models, *Environ. Sci. Technol.*, 2005, **39**(7), 1932–1942, DOI: 10.1021/es048917b.
78 F. Wegmann, L. Cavin, M. MacLeod, M. Scheringer and K. Hungerbuhler, The OECD software tool for screening chemicals for persistence and long-range transport potential, *Environ. Model. Software*, 2009, **24**(2), 228–237, DOI: 10.1016/j.envsoft.2008.06.014.
79 A. Hollander, M. Scheringer, V. Shatalov, E. Mantseva, A. Sweetman, M. Roemer, A. Baart, N. Suzuki, F. Wegmann and D. van de Meent, Estimating overall persistence and long-range transport potential of persistent organic pollutants: a comparison of seven multimedia mass balance models and atmospheric transport models, *J. Environ. Monit.*, 2008, **10**(10), 1139–1147, DOI: 10.1039/b803760d.